SCIENCE CHINA
Information Sciences

• RESEARCH PAPER •

April 2024, Vol. 67, Iss. 4, 142302:1–142302:17
https://doi.org/10.1007/s11432-023-3885-2

Impact of non-ideal UE hardware on cell-free massive MIMO network with centralized operation

Ning LI* & Pingzhi FAN

Institute of Mobile Communications, Southwest Jiaotong University, Chengdu 610031*, China*

Received 3 July 2023/Revised 27 September 2023/Accepted 27 October 2023/Published online 27 March 2024

Abstract This paper investigates the impact of non-ideal user equipment (UE) hardware on a cell-free (CF) massive MIMO (mMIMO) network with centralized operation under spatially correlated channels. The minimum mean-squared error (MMSE) estimator can be derived with the help of the generic non-ideal UE hardware model. It is demonstrated that even if the effective signal-to-noise ratio approaches infinity, pilot contamination and imperfect hardware can cause a non-zero estimation error floor. After that, a lower bound is determined for the ergodic uplink capacity of the centralized CF mMIMO network under non-ideal UE hardware. Moreover, the optimal receive combining vector is obtained to maximize the uplink spectral efficiency (SE). The maximum ratio (MR) and regularized zero-forcing (RZF) combining schemes are offered as alternatives in light of the computational complexity of the MMSE receiver. Comparing the RZF to the MMSE scheme under different levels of hardware impairments, our findings indicate that the RZF receiver suffers a negligible loss in total SE. For MR combining, a novel closed-form uplink achievable SE expression is obtained based on the MMSE estimator and the use-and-then-forget bounding technique. This expression gives vital insights into the achievable uplink performance with UE hardware impairments. Besides, for various hardware impairment factors, the impact of pilot sequence length on average sum SE is disclosed for different receive combining schemes. To increase the overall SE of the max-min fairness scheme, a heuristic fractional power control scheme with UE hardware impairments is developed, which can essentially avoid sacrificing the SE of other UEs while maximizing the SE of the unluckiest UE in the whole network. Finally, our theoretical performance analysis and power control algorithm are validated by simulation results, and fundamental design guidelines are provided for selecting hardware satisfying the practical UE requirements.

Keywords cell-free massive MIMO, centralized operation, spatially correlated channels, hardware impairments, channel estimation, uplink spectral efficiency, optimal receive combining, pilot length design, fractional power control

1 Introduction

Massive multiple-input multiple-output (mMIMO) is seen as a crucial technology for fifth-generation (5G) and future networks due to its ability to fulfill the exponentially growing need for high data rates [1–5]. By spatially multiplexing several user equipments (UEs), cellular networks may considerably enhance spectral efficiency (SE) [6, 7]. Cai et al. [8] examined multiple access schemes in cellular networks for large-scale Internet of Things (IoT) devices and presented two non-orthogonal multiple access approaches for short-packet transmissions in cellular IoT. Massive machine type communication for cellular networks has been investigated in [9], and a two-stage dynamic preamble selection assisted random access scheme is proposed. Recent research demonstrates that cell-free (CF) mMIMO may decrease fronthaul signaling and outperform conventional cellular mMIMO, enabling its implementation in the 6G network [10, 11]. The scalable CF mMIMO implementation architecture for the novel radio access network for 6G has been studied in [12], and relevant experimental results are given. The main operational idea is to simultaneously install a significant number of cooperative dispersed access points (APs) that cater to each UE. All APs are connected through an error-free fronthaul to a central processing unit (CPU) responsible for coordinating AP cooperation. Using the minimum mean square error (MMSE) receiver, Ref. [13] examined four distinct network architectures and demonstrated that CF mMIMO networks perform significantly better

* Corresponding author (email: lining@my.swjtu.edu.cn)

than small cell and conventional cellular mMIMO networks. A centralized approach with efficient MMSE processing dramatically reduces fronthaul signaling compared to distributed architectures and optimizes SE.

The majority of extant work in the CF mMIMO network concentrates on ideal transceiver hardware, which ignores the hardware impairments of the transmitter and receiver. However, hardware impairments influence actual wireless transceivers [14], such as phase noise, non-ideal analog filters, amplifier non-linearity, and quantization errors [6, 15]. Modeling the network with hardware impairments in [16] shows that mMIMO tolerates more significant hardware impairments, paving the way for deploying low-cost, high-efficiency antenna components. In mMIMO, the hardware distortion correlation may be safely ignored when there are many UEs [14]. This paper considers the centralized CF mMIMO network with non-ideal hardware in light of the aforementioned factors.

According to uncorrelated and correlated Rayleigh fading channels, the existing literature may be categorized into two groups. In the independent Rayleigh fading model, the analytical SE expressions for uplink transmission of a local CF mMIMO network under non-ideal hardware are obtained [17]. It is shown that the influence of hardware limitations on APs diminishes as the number of APs expands. Under ideal hardware conditions, the performance of the CF mMIMO network with zero-forcing (ZF) processing is analyzed in [18], indicating that the CF mMIMO network has significant potential in terms of SE compared to the traditional mMIMO network. In order to enhance the SE of wireless networks, the performance of non-orthogonal multiple access (NOMA)-assisted CF mMIMO networks under three linear precoders was investigated in [19], showing that NOMA-based CF mMIMO can support a larger number of UEs in comparison to the OMA-hybrid. To obtain higher spectral and energy efficiencies (SE-EE) in wireless networks, Ref. [20] investigated the full-duplex mode of CF mMIMO networks and presented an optimization algorithm to maximize SE and EE. Ref. [21] investigated the uplink transmission of the CF mMIMO network with hardware impairments, and two power application algorithms have been developed to optimize the sum SEs. The network performance under distributed mMIMO and small-cell operation have been studied in [22], with imperfect hardware and Doppler shift considered. The uplink achievable SE expression for imperfect hardware of the CF mMIMO network was obtained in [23], and an iterative power control technique to optimize the total SE was presented. Moreover, the physical layer security implications of hardware impairments in CF mMIMO networks have been investigated [24, 25]. In the correlated Rayleigh fading model, Ref. [26] investigated the influence of hardware impairments in scalable CF mMIMO networks and derived the uplink capacity bound that accounts for hardware impairments.

Unlike previous studies [17, 21, 23–25, 27, 28] that investigate uncorrelated Rayleigh fading channels, we want to concentrate on spatially correlated channels. Channels in practice are generally spatially correlated because the antennas have non-uniform radiation patterns that make it more probable for certain spatial directions to transmit strong signals [29]. Furthermore, there have been limited investigations on the impact of imperfect hardware on CF mMIMO network performance in correlated Rayleigh fading channels. The scalable CF mMIMO network with non-ideal hardware is studied in [26]. However, it is entirely different from the non-ideal UE hardware model considered in this paper, which is the UE hardware impairments cause hardware distortion and reduce the power of the signal term.

In [13, 30], it is shown that a centralized implementation not only dramatically reduces fronthaul signaling but also maximizes SE compared to distributed architectures. In light of this, this research focuses on the completely centralized CF mMIMO network. However, practical transceivers are inevitably affected by hardware impairments, whereas most previous studies have considered the hardware impairments of APs in the CF mMIMO network. Consequently, this paper will focus on the UE hardware impairments that are anticipated to have the most significant effect on the achievable SEs in the CF mMIMO network.

In contrast to the cellular network, CF mMIMO can offer nearly uniform high data rates service across the whole network [31]. In the CF mMIMO network, one of the vital optimization criteria is the max-min fairness power control scheme [32, 33]. Its purpose is to provide approximately the same SE for all UEs by maximizing the smallest SE among all UEs. However, this strategy will only help the most unfortunate UE at the expense of everyone else in the network [34–36]. In fact, most UEs hardly affect the most unfortunate UE in the CF mMIMO network. Based on [37], we design a fractional power control scheme for the centralized CF mMIMO network under non-ideal UE hardware.

To the best of our knowledge, this is the first work to offer an analytical investigation on the centralized CF mMIMO network with spatially correlated fading channels under non-ideal UE hardware. We will analyze and show how these hardware impairments affect channel estimation and achievable SE. The comparisons between this paper and relevant literature are summarized in Table 1 [13, 17, 23, 27, 28, 34].

Table 1 Comparisons between this work and relevant literature

Ref.	Non-ideal hardware	Correlated Channels	Centralized operation	MMSE processing	Pilot contamination	Closed-form	Max-min fairness
[13]	✗	✓	✓	✓	✓	✗	✓
[17]	✓	✗	✗	✗	✓	✓	✗
[23]	✓	✗	✗	✗	✓	✓	✗
[27]	✓	✗	✗	✗	✓	✓	✗
[28]	✓	✗	✗	✗	✗	✓	✓
[34]	✗	✗	✗	✗	✗	✓	✓
Proposed	✓	✓	✓	✓	✓	✓	✓

The following are the key contributions made by this paper:

• A well-established generic model is employed for UE hardware impairments in centralized CF mMIMO. Based on the MMSE estimator and the UE hardware impairments model, a closed-form channel estimation formula is derived, including the ideal hardware case [13] as a particular case.

• We derive the lower bound for the uplink ergodic capacity by utilizing the MMSE channel estimate with non-ideal UE hardware. Based on the obtained lower bound, we utilize the generalized Rayleigh quotient to determine the maximum SE and the optimal receive combining scheme for the CF mMIMO network in the presence of non-ideal UE hardware. In light of the high computational complexity of optimal receive combining, low-complexity maximum ratio (MR) and regularized ZF (RZF) combining schemes are presented for networks with non-ideal UE hardware.

• The closed-form expression for uplink achievable SE is derived with the help of MR combining using the use-and-then-forget (UatF) bounding technique, which provides essential insights into the achievable uplink performance under non-ideal UE hardware and guides the design of the network. Besides, for various hardware impairment factors, the impact of pilot sequence length on average sum SE is disclosed for different receive combining schemes.

• To increase the overall SE of the max-min fairness SE scheme, a heuristic fractional power control scheme with UE hardware impairments is presented, which can achieve almost the same SE for the most unfortunate UE without reducing the SE of other UEs in the whole network.

The structure of the remaining sections of this paper is as follows. Section 2 introduces a centralized CF mMIMO network with non-ideal UE hardware and discusses the uplink channel acquisition and data transmission processes. Section 3 presents the optimal receive combining vector that maximizes the SE, while also providing the low-complexity RZF and MR combining schemes. Section 3 also presents the UatF bound, which can deduce rigorous closed-form achievable SE expressions, and compares the max-min fairness and fractional power control schemes. The numerical performance comparisons are shown and discussed in Section 4. Section 5 concludes the paper with some remarks. The related proofs of this paper are included in the appendices.

Notation. Boldface lowercase and boldface uppercase letters are used in column vectors and matrices. $\boldsymbol{I}$ represents the identity matrix, while $\mathrm{diag}\left(\lambda_1, \ldots, \lambda_N\right)$ denotes a diagonal matrix with its main diagonal elements as $\lambda_1, \ldots, \lambda_N$. $\mathrm{tr}(\boldsymbol{X})$ corresponds to the trace of square matrix $\boldsymbol{X}$. Let $\boldsymbol{X}^*$ represent the complex conjugate operation of $\boldsymbol{X}$. $\boldsymbol{X}^{\mathrm{T}}$ and $\boldsymbol{X}^{\mathrm{H}}$ correspond to the transpose and Hermitian transpose operations of matrice $\boldsymbol{X}$. A complex Gaussian stochastic vector $\boldsymbol{x}$ is represented by $\mathcal{N}_{\mathbb{C}}(\boldsymbol{0}, \boldsymbol{R})$, where the mean is $\boldsymbol{0}$ and $\boldsymbol{R}$ denotes the correlation matrix. The expected value of a stochastic vector $\boldsymbol{x}$ is indicated by $\mathbb{E}\left\{\boldsymbol{x}\right\}$.

2 Network model

The evolution from the conventional cellular mMIMO network to the CF mMIMO network is shown in Figure 1. Each UE in a cellular mMIMO network is linked to one base station (BS) that provides service to it, as illustrated in Figure 1(a). A centralized CF mMIMO network under non-ideal UE hardware is investigated in this paper, where K UEs with a single antenna can connect to L dispersed APs, and N antennas in total are installed on each AP. Each AP is then connected to the CPU through the fronthaul with unlimited-capacity, and the network model is demonstrated in Figure 1(b). Directly connecting all APs to the CPU might not be scalable, especially in large networks with numerous APs. A hierarchical network topology that uses intermediate APs as relays can provide better scalability. With the help of the non-ideal UE hardware model established in [6, 15], the UE hardware impairments may be characterized as the intended signal power of ideal hardware multiplied by $\sqrt{1-\epsilon^2}$, where $0 \leqslant \epsilon < 1$ and the Gaussian

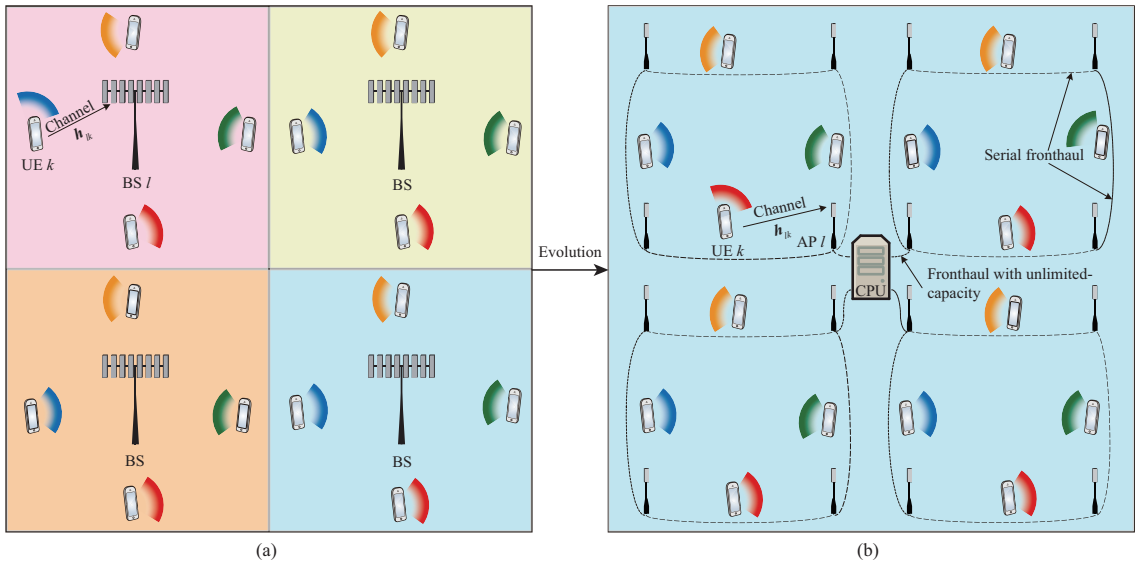

Figure 1 Illustration of evolution from cellular mMIMO network to CF mMIMO network. (a) Cellular mMIMO network; (b) CF mMIMO network.

distortion term is added. ϵ represents the level of hardware impairments and is known as the hardware impairment factor. The typical values are in the range $0 \leqslant \epsilon \leqslant 0.17$ in long term evolution (LTE) [38], where $\epsilon = 0$ represents ideal UE hardware, and $\epsilon = 1$ is the pathological case. It is anticipated that UE hardware impairments would be the primary factor limiting achievable SEs [16], so this paper only considers UE hardware impairments in CF mMIMO networks. The spatially correlated channel from UE k to AP l is denoted as $\boldsymbol{h}_{lk} \in \mathbb{C}^N$. According to the standard block fading channel model [29], $\boldsymbol{h}_{lk}$ is constant and frequency-flat in each coherence block. A spatially correlated Rayleigh fading model describes the channel response as

$$\boldsymbol{h}_{lk} \sim \mathcal{N}_{\mathbb{C}}(\boldsymbol{0}, \boldsymbol{R}_{lk}), \tag{1}$$

where $\boldsymbol{R}_{lk} \in \mathbb{C}^{N \times N}$ describes the spatial correlation of the channel $\boldsymbol{h}_{lk}$, and the large-scale fading is described as $\beta_{lk} \triangleq \mathrm{tr}(\boldsymbol{R}_{lk})/N$. This study concentrates on the uplink transmission, which comprises τ_p samples for pilots and $\tau_c - \tau_p$ samples for uplink data signals, where τ_c represents the number of samples within each coherence block. Next, we will analyze how non-ideal UE hardware affects the performance of a centralized CF mMIMO network.

2.1 Uplink channel estimation

Assuming that UE i transmits an uplink data signal with average power $\mathbb{E}\{|s_i|^2\} = p_i$. The non-ideal UE hardware model described in [15] is used to generate $\sqrt{1-\epsilon^2}s_i + e_i$, which is transmitted over the channel in place of s_i, where $e_i \sim \mathcal{N}_{\mathbb{C}}(0, \epsilon^2 p_i)$ represents the uplink distortion noise induced by UE i and is uncorrelated with s_i. Unlike conventional receiver noise, the distortion power is dependent on the input signal power p_i. Therefore, the UE hardware distortion becomes the primary limiting factor for performance in situations with a high signal-to-noise ratio (SNR). It is presumed for channel acquisition that the network utilizes τ_p mutually orthogonal pilots $\boldsymbol{\phi}_1, \ldots, \boldsymbol{\phi}_{\tau_p}$. The pilot of UE k can be represented by $\boldsymbol{\phi}_k \in \mathbb{C}^{\tau_p}$ with $\|\boldsymbol{\phi}_k\|^2 = \tau_p$. These orthogonal pilots are distributed among K UEs such that the pilot reuse pattern is

$$\boldsymbol{\phi}_i^{\mathrm{H}} \boldsymbol{\phi}_k = \begin{cases} \tau_p, & \text{if } i \in \mathcal{P}_k, \\ 0, & \text{if } i \notin \mathcal{P}_k. \end{cases} \tag{2}$$

For a massive access network $K > \tau_p$, multiple UEs may be allocated the same pilot signal. Thus the set is defined as

$$\mathcal{P}_k = \{i : \boldsymbol{\phi}_i = \boldsymbol{\phi}_k, i = 1, \ldots, K\}, \tag{3}$$

which comprises the indices of all UEs using the same pilot signal as UE k. The received uplink pilot signal $\boldsymbol{Y}_l^p \in \mathbb{C}^{N\times\tau_p}$ at AP l in the pilot transmission phase can be provided by

$$\boldsymbol{Y}_l^p = \sum_{i=1}^{K} \boldsymbol{h}_{li}\left(\sqrt{p_i\left(1-\epsilon^2\right)}\boldsymbol{\phi}_i^{\mathrm{T}} + \boldsymbol{e}_i^{\mathrm{T}}\right) + \boldsymbol{N}_l^p, \tag{4}$$

where the transmitter distortion is represented by $\boldsymbol{e}_i \sim \mathcal{N}_{\mathbb{C}}(\boldsymbol{0}_{\tau_p}, \epsilon^2 p_i \boldsymbol{I}_{\tau_p})$. The additive receiver noise is $\boldsymbol{N}_l^p \in \mathbb{C}^{N\times\tau_p}$, where the distribution of each element is $\mathcal{N}_{\mathbb{C}}\left(0,\sigma^2\right)$. To estimate $\boldsymbol{h}_{lk}$, the AP l can multiply $\boldsymbol{Y}_l^p$ with the pilot $\boldsymbol{\phi}_k$ to obtain the signal $\boldsymbol{y}_{lk}^p \in \mathbb{C}^N$ as

$$\boldsymbol{y}_{lk}^p = \boldsymbol{Y}_l^p\boldsymbol{\phi}_k^* = \sqrt{p_k\left(1-\epsilon^2\right)}\tau_p\boldsymbol{h}_{lk} + \sum_{i=1}^{K}\boldsymbol{h}_{li}\boldsymbol{e}_i^{\mathrm{T}}\boldsymbol{\phi}_k^* + \sum_{i\in\mathcal{P}_k\setminus\{k\}}\sqrt{p_i\left(1-\epsilon^2\right)}\tau_p\boldsymbol{h}_{li} + \boldsymbol{N}_l^p\boldsymbol{\phi}_k^*. \tag{5}$$

The estimated value of $\boldsymbol{h}_{lk}$ will be derived from the processed signal $\boldsymbol{y}_{lk}^p$ above. Since the distortion is not orthogonal to the pilot sequence, the distortion of all UE transmitters affects $\boldsymbol{y}_{lk}^p$. The MMSE estimate of $\boldsymbol{h}_{lk}$ is calculated as follows.

Lemma 1. Under non-ideal UE hardware, the MMSE estimator of $\boldsymbol{h}_{lk}$ on the basis of the observation $\boldsymbol{y}_{lk}^p$ is

$$\hat{\boldsymbol{h}}_{lk} = \sqrt{p_k\left(1-\epsilon^2\right)}\boldsymbol{R}_{lk}\boldsymbol{\Psi}_{lk}^{-1}\boldsymbol{y}_{lk}^p, \tag{6}$$

where

$$\boldsymbol{\Psi}_{lk} = \sum_{i\in\mathcal{P}_k} p_i\left(1-\epsilon^2\right)\tau_p\boldsymbol{R}_{li} + \sum_{i=1}^{K}\epsilon^2 p_i\boldsymbol{R}_{li} + \sigma^2\boldsymbol{I}_N. \tag{7}$$

The channel estimation $\hat{\boldsymbol{h}}_{lk}$ and estimation error $\tilde{\boldsymbol{h}}_{lk} = \boldsymbol{h}_{lk} - \hat{\boldsymbol{h}}_{lk}$ are uncorrelated, and their distributions are $\hat{\boldsymbol{h}}_{lk} \sim \mathcal{N}_{\mathbb{C}}\left(\boldsymbol{0}, \boldsymbol{R}_{lk} - \boldsymbol{C}_{lk}\right)$ and $\tilde{\boldsymbol{h}}_{lk} \sim \mathcal{N}_{\mathbb{C}}\left(\boldsymbol{0}, \boldsymbol{C}_{lk}\right)$, respectively, where the estimation error covariance matrix is

$$\boldsymbol{C}_{lk} = \mathbb{E}\{\tilde{\boldsymbol{h}}_{lk}\tilde{\boldsymbol{h}}_{lk}^{\mathrm{H}}\} = \boldsymbol{R}_{lk} - p_k\left(1-\epsilon^2\right)\tau_p\boldsymbol{R}_{lk}\boldsymbol{\Psi}_{lk}^{-1}\boldsymbol{R}_{lk}. \tag{8}$$

Proof. The detailed proof can be found in Appendix A.

Compared to the channel estimation of the ideal UE hardware [13], the transmission power of UE k can be reduced from p_k to $p_k(1-\epsilon^2)$. Moreover, matrix $\boldsymbol{\Psi}_{lk}$ contains an additional term of hardware distortion resulting from UE hardware impairments in comparison to perfect hardware. Note that equation (6) simplifies to [13, Eq. (4)] in the special case of perfect hardware.

2.2 Uplink network model

The signal $\boldsymbol{y}_l \in \mathbb{C}^N$ received at AP l during the uplink data transfer can be represented as

$$\boldsymbol{y}_l = \sum_{i=1}^{K}\boldsymbol{h}_{li}\left(\sqrt{1-\epsilon^2}s_i + e_i\right) + \boldsymbol{n}_l. \tag{9}$$

The AP l can obtain the decoded signal of UE k by taking the inner product of the decoding vector $\boldsymbol{v}_{lk}$ and $\boldsymbol{y}_l$ as

$$\hat{s}_{lk} = \boldsymbol{v}_{lk}^{\mathrm{H}}\boldsymbol{y}_l. \tag{10}$$

After receiving the data estimates from each AP, the CPU finally decodes the signal of UE k as

$$\hat{s}_k = \sum_{l=1}^{L}\hat{s}_{lk} = \sum_{l=1}^{L}\boldsymbol{v}_{lk}^{\mathrm{H}}\boldsymbol{y}_l = \boldsymbol{v}_k^{\mathrm{H}}\boldsymbol{y}, \tag{11}$$

where $\boldsymbol{v}_k = [\boldsymbol{v}_{1k}^{\mathrm{T}}, \ldots, \boldsymbol{v}_{Lk}^{\mathrm{T}}]^{\mathrm{T}} \in \mathbb{C}^{LN}$ indicates the collective combining vector in centralized operation, and the CPU receives a signal that may be described as

$$\boldsymbol{y} = \begin{bmatrix}\boldsymbol{y}_1\\ \vdots\\ \boldsymbol{y}_L\end{bmatrix} = \sum_{i=1}^{K}\boldsymbol{h}_i\left(\sqrt{1-\epsilon^2}s_i + e_i\right) + \boldsymbol{n}, \tag{12}$$

where $\boldsymbol{h}_i = [\boldsymbol{h}_{1i}^{\mathrm{T}}, \ldots, \boldsymbol{h}_{Li}^{\mathrm{T}}]^{\mathrm{T}}$ denotes the collective channel response, and $\boldsymbol{n} = [\boldsymbol{n}_1^{\mathrm{T}}, \ldots, \boldsymbol{n}_L^{\mathrm{T}}]^{\mathrm{T}} \in \mathbb{C}^{LN}$ represents the collective noise. The collective channel distribution of UE k can be denoted by $\boldsymbol{h}_k \sim \mathcal{N}_{\mathbb{C}}(\boldsymbol{0}, \boldsymbol{R}_k)$, where $\boldsymbol{R}_k = \mathrm{diag}(\boldsymbol{R}_{1k}, \ldots, \boldsymbol{R}_{Lk}) \in \mathbb{C}^{LN \times LN}$ represents a block-diagonal matrix with the spatial correlation matrices $\boldsymbol{R}_{1k}, \ldots, \boldsymbol{R}_{Lk}$ on the diagonal. Suppose the CPU knows the distribution of $\hat{\boldsymbol{h}}_k$ as $\hat{\boldsymbol{h}}_k \sim \mathcal{N}_{\mathbb{C}}\left(\boldsymbol{0}, p_k\left(1-\epsilon^2\right)\tau_p \boldsymbol{R}_k \boldsymbol{\Psi}_k^{-1} \boldsymbol{R}_k\right)$, where $\boldsymbol{\Psi}_k^{-1} = \mathrm{diag}\left(\boldsymbol{\Psi}_{1k}^{-1}, \ldots, \boldsymbol{\Psi}_{Lk}^{-1}\right)$. The distribution of the estimation error $\tilde{\boldsymbol{h}}_k$ is $\tilde{\boldsymbol{h}}_k \sim \mathcal{N}_{\mathbb{C}}(\boldsymbol{0}, \boldsymbol{C}_k)$ with $\boldsymbol{C}_k = \mathrm{diag}(\boldsymbol{C}_{1k}, \ldots, \boldsymbol{C}_{Lk})$. After that, this work attempts to determine the optimal receive combining vector for a centralized CF mMIMO network under non-ideal UE hardware.

3 Uplink spectral efficiency

In this section, we want to reveal the optimal receive combining vector to maximize the uplink SE. The first step is to rewrite (11) by inserting (12) into (11) as

$$\hat{s}_k = \boldsymbol{v}_k^{\mathrm{H}} \hat{\boldsymbol{h}}_k \sqrt{1-\epsilon^2} s_k + \boldsymbol{v}_k^{\mathrm{H}} \tilde{\boldsymbol{h}}_k \sqrt{1-\epsilon^2} s_k + \sum_{i=1, i \neq k}^{K} \boldsymbol{v}_k^{\mathrm{H}} \boldsymbol{h}_i \sqrt{1-\epsilon^2} s_i + \sum_{i=1}^{K} \boldsymbol{v}_k^{\mathrm{H}} \boldsymbol{h}_i e_i + \boldsymbol{v}_k^{\mathrm{H}} \boldsymbol{n}, \tag{13}$$

where the desired signal can be split into two parts based on the estimated channel $\hat{\boldsymbol{h}}_k$ and the estimation error $\tilde{\boldsymbol{h}}_k$. Next, we will determine the lower bound on the ergodic uplink capacity and find the optimal receive combining vector.

3.1 Optimal receive combining scheme

The following findings are derived by taking the first term of the equation in (13) as the desired component and the other four as interference in the receiver.

Theorem 1. According to MMSE channel estimation, the lower bound for the ergodic uplink capacity of UE k is

$$\mathsf{C} \geqslant \mathsf{SE}_k = \frac{\tau_u}{\tau_c} \mathbb{E}\left\{\log_2\left(1 + \mathsf{SINR}_k\right)\right\}, \tag{14}$$

with

$$\mathsf{SINR}_k = \frac{p_k (1-\epsilon^2) \left|\boldsymbol{v}_k^{\mathrm{H}} \hat{\boldsymbol{h}}_k\right|^2}{\boldsymbol{v}_k^{\mathrm{H}} \left(\sum_{i=1}^{K} p_i (\hat{\boldsymbol{h}}_i \hat{\boldsymbol{h}}_i^{\mathrm{H}} + \boldsymbol{C}_i) + \boldsymbol{Z}_k\right) \boldsymbol{v}_k}, \tag{15}$$

where

$$\boldsymbol{Z}_k = p_k\left(\epsilon^2 - 1\right) \hat{\boldsymbol{h}}_k \hat{\boldsymbol{h}}_k^{\mathrm{H}} + \sigma^2 \boldsymbol{I}_{LN}. \tag{16}$$

and the expectation operation is for the channel estimates.

Proof. The detailed proof can be found in Appendix B.

The achievable uplink SE for a centralized CF mMIMO network under non-ideal UE hardware is represented by the lower channel capacity bound shown in Theorem 1. $\frac{\tau_u}{\tau_c}$ represents the ratio of samples used for uplink data transmission per coherence block. Therefore, the pre-log factor $\frac{\tau_u}{\tau_c}$ can be increased by shortening the length of the pilot. To maximize the SE in Theorem 1, the optimal receive combining scheme is provided in Corollary 1.

Corollary 1. The optimal receive combining scheme is

$$\boldsymbol{v}_k^{\mathrm{MMSE}} = \left(\sum_{i=1}^{K} p_i \left(\hat{\boldsymbol{h}}_i \hat{\boldsymbol{h}}_i^{\mathrm{H}} + \boldsymbol{C}_i\right) + \sigma^2 \boldsymbol{I}_{LN}\right)^{-1} \hat{\boldsymbol{h}}_k, \tag{17}$$

which results in the maximized uplink instantaneous SINR as

$$\mathsf{SINR}_k = p_k\left(1-\epsilon^2\right) \hat{\boldsymbol{h}}_k^{\mathrm{H}} \left(\sum_{i=1}^{K} p_i \left(\hat{\boldsymbol{h}}_i \hat{\boldsymbol{h}}_i^{\mathrm{H}} + \boldsymbol{C}_i\right) + \boldsymbol{Z}_k\right)^{-1} \hat{\boldsymbol{h}}_k. \tag{18}$$

Proof. The detailed proof can be found in Appendix C.

Recall that the hardware impairment factor ϵ affects the channel estimation, and Corollary 1 provides the optimal combining vector with UE hardware impairments. Since Eq. (17) can minimize MSE $\mathbb{E}\{|s_k-\hat{s}_k|^2|\{\hat{\boldsymbol{h}}_i\}\}$ during data decoding, it is referred to as the MMSE combining scheme with non-ideal UE hardware. Due to the high computational complexity of MMSE combining, we want to discover an alternate receive combining strategy to minimize the complexity without considerably compromising the network performance. In general, when the interfering UEs in the CF mMIMO network have good channel conditions, then all the covariance matrices of the estimation error in (17) may be ignored to obtain

$$\boldsymbol{v}_k^{\mathrm{RZF}}=\left(\sum_{i=1}^{K}p_i\hat{\boldsymbol{h}}_i\hat{\boldsymbol{h}}_i^{\mathrm{H}}+\sigma^2\boldsymbol{I}_{LN}\right)^{-1}\hat{\boldsymbol{h}}_k, \tag{19}$$

which is referred to as the RZF combining scheme with non-ideal UE hardware. In addition, the MR receive combining scheme $\boldsymbol{v}_k^{\mathrm{MR}}=\hat{\boldsymbol{h}}_k$ is used as a benchmark, which maximizes the desired signal $|\boldsymbol{v}_k^{\mathrm{H}}\hat{\boldsymbol{h}}_k|^2$ in (15). The MR combining has the lowest computational complexity since $\hat{\boldsymbol{h}}_k$ is employed as the combining vector. The Monte Carlo methodology can be utilized to simulate the SE in Theorem 1. However, the rigorous closed-form expression of the achievable SE is required to offer accurate insights into the CF mMIMO network under non-ideal UE hardware over spatially correlated channels. The following is the UatF bounding technique that may be used to derive accurate achievable closed-form SE expressions.

3.2 Lower capacity bound

The channel estimate is employed in the computation of the receive combining schemes, however, this channel estimate information is not utilized in the signal detection process. Specifically, we rewrite the final decoded signal in (13) by adding and subtracting $\sqrt{1-\epsilon^2}\mathbb{E}\left\{\boldsymbol{v}_k^{\mathrm{H}}\boldsymbol{h}_k\right\}s_k$ as

$$\begin{aligned}\hat{s}_k=&\sqrt{1-\epsilon^2}\mathbb{E}\left\{\boldsymbol{v}_k^{\mathrm{H}}\boldsymbol{h}_k\right\}s_k+\sqrt{1-\epsilon^2}\left(\boldsymbol{v}_k^{\mathrm{H}}\boldsymbol{h}_k-\mathbb{E}\left\{\boldsymbol{v}_k^{\mathrm{H}}\boldsymbol{h}_k\right\}\right)s_k\\&+\sum_{i=1,i\neq k}^{K}\boldsymbol{v}_k^{\mathrm{H}}\boldsymbol{h}_i\sqrt{1-\epsilon^2}s_i+\sum_{i=1}^{K}\boldsymbol{v}_k^{\mathrm{H}}\boldsymbol{h}_ie_i+\boldsymbol{v}_k^{\mathrm{H}}\boldsymbol{n},\end{aligned} \tag{20}$$

where $\sqrt{1-\epsilon^2}\mathbb{E}\left\{\boldsymbol{v}_k^{\mathrm{H}}\boldsymbol{h}_k\right\}s_k$ is regarded as the true desired signal, while the remaining four terms are considered as interference. As an alternative to Theorem 1, we adopt the UatF bounding technique [29], which can lead to a closed form of SE as follows.

Theorem 2. Based on using the UatF bounding technique, the lower bound for the ergodic uplink capacity of UE k is

$$\underline{\mathsf{C}}\geqslant\underline{\mathsf{SE}}_k=\frac{\tau_u}{\tau_c}\log_2\left(1+\underline{\mathsf{SINR}}_k\right), \tag{21}$$

with

$$\underline{\mathsf{SINR}}_k=\frac{D_k}{\sum_{i=1}^{K}p_i\mathbb{E}\{|\boldsymbol{v}_k^{\mathrm{H}}\boldsymbol{h}_i|^2\}-D_k+\sigma^2\mathbb{E}\{\|\boldsymbol{v}_k\|^2\}}, \tag{22}$$

where

$$D_k=p_k\left(1-\epsilon^2\right)\left|\mathbb{E}\left\{\boldsymbol{v}_k^{\mathrm{H}}\boldsymbol{h}_k\right\}\right|^2, \tag{23}$$

and expectation operation is for the channel realizations.

Proof. The detailed proof can be found in Appendix D.

Due to the fact that the channel estimations are not utilized for signal detection, the SE provided by Theorem 2 is intuitively less tight than the SE provided by Theorem 1. However, Theorem 2 can lead to the SE expressed in closed form. By individually calculating the expectations of the denominator and numerator in (22) with the help of MR combining, the SE can be given in closed form as follows.

Corollary 2. Based on MMSE channel estimation, if MR combining scheme with $\boldsymbol{v}_k=\hat{\boldsymbol{h}}_k$ is utilized, then

$$\mathbb{E}\left\{\boldsymbol{v}_k^{\mathrm{H}}\boldsymbol{h}_k\right\}=p_k\left(1-\epsilon^2\right)\tau_p\sum_{l=1}^{L}\mathrm{tr}(\boldsymbol{R}_{lk}\boldsymbol{\Psi}_{lk}^{-1}\boldsymbol{R}_{lk}), \tag{24}$$

$$\mathbb{E}\{\|\boldsymbol{v}_k\|^2\} = p_k\left(1-\epsilon^2\right)\tau_p\sum_{l=1}^{L}\mathrm{tr}(\boldsymbol{R}_{lk}\boldsymbol{\Psi}_{lk}^{-1}\boldsymbol{R}_{lk}), \tag{25}$$

and

$$\begin{aligned}\mathbb{E}\left\{\left|\boldsymbol{v}_k^{\mathrm{H}}\boldsymbol{h}_i\right|^2\right\} =& p_k\left(1-\epsilon^2\right)\tau_p\sum_{l=1}^{L}\mathrm{tr}\left(\boldsymbol{R}_{li}\boldsymbol{R}_{lk}\boldsymbol{\Psi}_{lk}^{-1}\boldsymbol{R}_{lk}\right)\\ &+\begin{cases}p_k p_i\left(1-\epsilon^2\right)^2\tau_p^2\left|\sum_{l=1}^{L}\mathrm{tr}\left(\boldsymbol{R}_{li}\boldsymbol{\Psi}_{lk}^{-1}\boldsymbol{R}_{lk}\right)\right|^2, & i\in\mathcal{P}_k,\\ 0, & i\notin\mathcal{P}_k.\end{cases}\end{aligned} \tag{26}$$

So the expression for $\underline{\mathsf{SINR}}_k$ in (21) becomes

$$\begin{aligned}\underline{\mathsf{SINR}}_k =& \left\{p_k^2\left(1-\epsilon^2\right)^2\tau_p d\right\}\Big/\left\{\frac{1}{d}\sum_{i=1}^{K}\sum_{l=1}^{L}p_i\mathrm{tr}\left(\boldsymbol{R}_{li}\boldsymbol{R}_{lk}\boldsymbol{\Psi}_{lk}^{-1}\boldsymbol{R}_{lk}\right)\right.\\ &\left.+\frac{1}{d}\sum_{i\in\mathcal{P}_k\setminus\{k\}}p_i^2\left(1-\epsilon^2\right)\tau_p\left|\sum_{l=1}^{L}\mathrm{tr}\left(\boldsymbol{R}_{li}\boldsymbol{\Psi}_{lk}^{-1}\boldsymbol{R}_{lk}\right)\right|^2+p_k^2\tau_p\left(1-\epsilon^2\right)\epsilon^2 d+\sigma^2\right\},\end{aligned} \tag{27}$$

where

$$d = \sum_{l=1}^{L}\mathrm{tr}\left(\boldsymbol{R}_{lk}\boldsymbol{\Psi}_{lk}^{-1}\boldsymbol{R}_{lk}\right). \tag{28}$$

To show the impact of spatial correlation, we set $\boldsymbol{R}_{li}=\beta_{li}\boldsymbol{I}_N$ as a special case of spatially uncorrelated fading, then Eq. (27) simplifies to

$$\underline{\mathsf{SINR}}_k = \frac{p_k^2\left(1-\epsilon^2\right)^2\tau_p f_k^2 N}{\sum_{i=1}^{K}\sum_{l=1}^{L}p_i\beta_{li}\beta_{lk}^2\psi_{lk}^{-1}+\sum_{i\in\mathcal{P}_k\setminus\{k\}}p_i^2\left(1-\epsilon^2\right)\tau_p f_i^2 N+p_k^2\tau_p\left(1-\epsilon^2\right)\epsilon^2 f_k^2 N+\sigma^2 f_k}, \tag{29}$$

where

$$f_i = \sum_{l=1}^{L}\beta_{li}\beta_{lk}\psi_{lk}^{-1}, \tag{30}$$

$$\psi_{lk} = \sum_{i\in\mathcal{P}_k}p_i\left(1-\epsilon^2\right)\tau_p\beta_{li}+\sum_{i=1}^{K}\epsilon^2 p_i\beta_{li}+\sigma^2. \tag{31}$$

Proof. The detailed proof can be found in Appendix E.

The Corollary 2 provides essential insights about the achievable uplink SE. In accordance with the estimation error covariance matrix $\boldsymbol{C}_{lk}$ in (8), the signal term in the numerator of (27) is

$$p_k^2\tau_p\left(1-\epsilon^2\right)^2 d = p_k\left(1-\epsilon^2\right)\sum_{l=1}^{L}\mathrm{tr}\left(\boldsymbol{R}_{lk}-\boldsymbol{C}_{lk}\right), \tag{32}$$

which represents the sum of the channel estimation correlation matrix traces from all APs servicing UE k, multiplied by the scaled transmission power $p_k\left(1-\epsilon^2\right)$. Consequently, the signal strength is dependent on both the accuracy of the channel estimate and the hardware quality. In the special case of uncorrelated fading, the signal term is $p_k^2\left(1-\epsilon^2\right)^2\tau_p f_k^2 N$, which increases linearly with N. There are four terms in the denominator of the expression (27). The first item represents the summation across all UEs, where UE i generates interference $\frac{1}{d}\sum_{l=1}^{L}p_i\mathrm{tr}\left(\boldsymbol{R}_{li}\boldsymbol{R}_{lk}\boldsymbol{\Psi}_{lk}^{-1}\boldsymbol{R}_{lk}\right)$. For uncorrelated fading, it is easy to see that it does not increase linearly with N, so called non-coherent interference. In spatially correlated channels, one can reduce interference by setting more considerable angle differences between UEs. For example, in the extreme case of $\boldsymbol{R}_{li}\boldsymbol{R}_{lk}=\boldsymbol{0}_{N\times N}$, there can be no interference between two UEs. The second term

Algorithm 1 Fixed-point algorithm for the solution of the max-min fairness SE with UE hardware impairments problem in (33)

Input: a_k, $\boldsymbol{b}_k$, σ_k^2, ϵ, τ_u/τ_c, K, $p_{\max}$, the solution accuracy δ;
Output: Max-min fairness SE $\min_{k\in\{1,\ldots,K\}} \frac{\tau_u}{\tau_c}\log_2\left(1+\underline{\mathsf{SINR}}_k\left(\boldsymbol{p}\right)\right)$, optimal uplink transmission powers $\boldsymbol{p}$;
`/* Initialization */`
Set the solution accuracy $\delta > 0$ and arbitrary initial power $\boldsymbol{p} > \boldsymbol{0}_K$;
Compute a_k, $\boldsymbol{b}_k$, and σ_k^2 based on the receive combining scheme $\boldsymbol{v}_k$ and the hardware impairment factor ϵ;
`/* Fixed-point algorithm for max-min SE fairness */`
while $\max_{k\in\{1,\ldots,K\}} \underline{\mathsf{SINR}}_k\left(\boldsymbol{p}\right) - \min_{k\in\{1,\ldots,K\}} \underline{\mathsf{SINR}}_k\left(\boldsymbol{p}\right) > \delta$ **do**
  • $p_k \leftarrow p_k / \underline{\mathsf{SINR}}_k\left(\boldsymbol{p}\right)$, $k = 1,\ldots,K$;
  • $\boldsymbol{p} \leftarrow \frac{p_{\max}}{\max_{k\in\{1,\ldots,K\}} p_k}\boldsymbol{p}$;
  • denominator $\leftarrow \boldsymbol{p}^{\mathrm{T}} * \boldsymbol{b}_k + \sigma_k^2$;
  • $\underline{\mathsf{SINR}}_k(\boldsymbol{p}) \leftarrow \frac{\boldsymbol{p}*(1-\epsilon^2)a_k}{\text{denominator}}$;
end while

resulting from pilot contamination is the presence of UEs in $\mathcal{P}_k \setminus \{k\}$. In the special case of uncorrelated fading, it can be observed that it increases linearly with N. Self-distortion is the third term produced by the intended UE distorting itself when there are hardware impairments. Note that the third term disappears when the hardware is ideal by simply setting $\epsilon = 0$. The fourth term is the total receiver noise power. After that, we evaluate the effect of imperfect UE hardware on channel estimation and SE through numerical simulations, hoping to yield essential insights into CF mMIMO network design.

3.3 Max-min fairness

The purpose of max-min fairness in a CF mMIMO network is to achieve complete fairness by enhancing the performance of the weakest UE. Hence, this method guarantees that all UEs have the same performance. We define $\boldsymbol{p} = [p_1,\ldots,p_k]^{\mathrm{T}}$ as the collection of uplink powers for all UEs. Therefore, the max-min fairness SE optimization problem for the centralized CF mMIMO network with non-ideal UE hardware can be given in its general form as

$$\begin{aligned} &\underset{\boldsymbol{p}\geqslant 0_K}{\text{maximize}} \quad \min_{k\in\{1,\ldots,K\}} \quad \frac{\tau_u}{\tau_c}\log_2\left(1+\frac{p_k\left(1-\epsilon^2\right)a_k}{\boldsymbol{p}^{\mathrm{T}}\boldsymbol{b}_k+\sigma_k^2}\right) \\ &\text{subject to} \;\; 0 \leqslant p_k \leqslant p_{\max},\; k=1,\ldots,K, \end{aligned} \tag{33}$$

with

$$a_k = \left|\mathbb{E}\left\{\boldsymbol{v}_k^{\mathrm{H}}\boldsymbol{h}_k\right\}\right|^2, \tag{34}$$

$$\sigma_k^2 = \sigma^2\mathbb{E}\{\|\boldsymbol{v}_k\|^2\}, \tag{35}$$

$$b_{ki} = \begin{cases} \mathbb{E}\{\left|\boldsymbol{v}_k^{\mathrm{H}}\boldsymbol{h}_i\right|^2\}, & i \neq k, \\ \mathbb{E}\{\left|\boldsymbol{v}_k^{\mathrm{H}}\boldsymbol{h}_k\right|^2\} - \left(1-\epsilon^2\right)a_k, & i = k. \end{cases} \tag{36}$$

Note that maximizing the minimum value of $\underline{\mathsf{SE}}_k$ for UE k in (33) is equivalent to maximizing the minimum value of $\underline{\mathsf{SINR}}_k = p_k\left(1-\epsilon^2\right)a_k/\left(\boldsymbol{p}^{\mathrm{T}}\boldsymbol{b}_k+\sigma_k^2\right)$, where the vector $\boldsymbol{b}_k = [b_{k1},\ldots,b_{kK}]^{\mathrm{T}}$ is the average channel gains of the interfering signals for the UE k. $\underline{\mathsf{SINR}}_k$ is inversely proportional to the transmission power $\boldsymbol{p}$ of other UEs and proportionate to the transmission power p_k of UE k. Since the SE of UE k is related to its own transmission power p_k and the interference power from other UEs, it conflicts with the SE of other UEs. To address the max-min fair SE problem in (33), we developed a fixed-point algorithm for UE hardware impairments in Algorithm 1 on the fixed-point algorithm in [39]. It can converge to the optimum max-min fairness issue solution in (33) for different hardware impairment factors. All UEs will have almost identical SE, and at least one will transmit at full power $p_{\max}$. Because Algorithm 1 only requires repetitive closed-form updates of variables, the convergence speed is fast, and the computational complexity is relatively low. It can be seen that the computational complexity of Algorithm 1 is dependent on the complexity of calculating the SE of each UE and the number of iterations, while the complexity of computing the SE of each UE depends on the number of UEs, the number of APs, channel estimation, and the receive combining scheme.

However, The max-min fairness only considers the UE with the lowest SE at the expense of everyone else. The most unfortunate UE is hardly affected by the majority of UEs in the network but will cause the plurality of UEs to be forced to reduce their transmit power. Based on [40], we offer a fractional

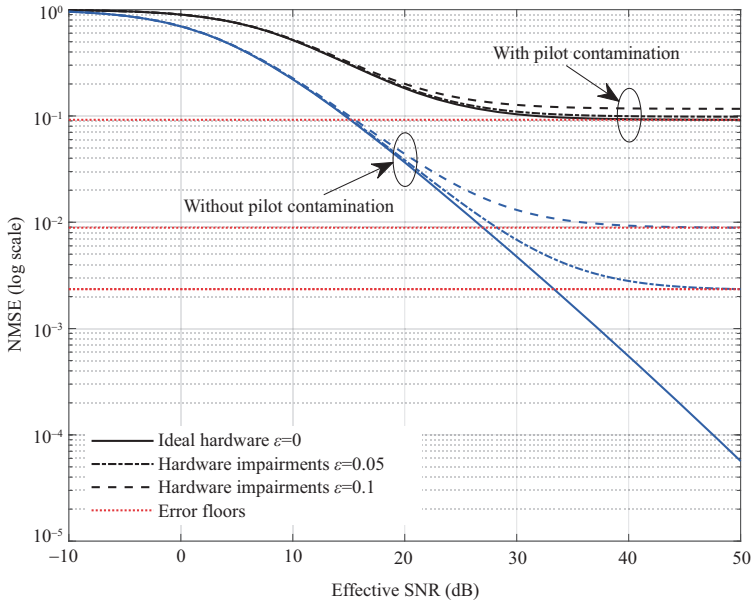

Figure 2 NMSE of channel estimation for spatially correlated channels under different hardware impairment levels, where a pilot length is 10 with pilot contamination and 40 without pilot contamination.

power control scheme for the centralized CF mMIMO network under non-ideal UE hardware, in which UE k chooses its uplink to transmit power according to the following expression:

$$p_k = p_{\max} \frac{\left(\sum_{l=1}^{L} \beta_{lk}\right)^{v}}{\max_{i \in \{1,\ldots,K\}} \left(\sum_{l=1}^{L} \beta_{li}\right)^{v}}, \tag{37}$$

where the power control behavior is shown by the exponent v. All UEs will transmit at full power $p_{\max}$ if $v = 0$. If $v = -1$, an approximate version of max-min fairness power control may be observed. By choosing the value of $v \in [-1, 0]$ considered in (37), individual SE utility functions may be heuristically optimized.

4 Numerical results and performance comparison

This section shows numerically how the non-ideal UE hardware impacts the centralized CF mMIMO network performance. For a fair comparison, we follow the same parameter configurations in [13, 39], where $L = 100$ APs and $K = 40$ UEs are allocated in an area of 1×1 km square, with $N = 4$ antennas setup on each AP. The large-scale fading coefficient β_{lk} can be described as $\beta_{lk}\,[\text{dB}] = -30.5 - 36.7 \log_{10}(d_{lk}/1\,\text{m}) + F_{lk}$, where d_{lk} indicates the distance from UE k to AP l and $F_{lk} \sim \mathcal{N}(0, 4^2)$ stands for the shadow fading [41]. The comparable Rayleigh fading and propagation model as [39] is utilized. In the network parameter setting, we suppose that $p_k = 100$ mW, $\tau_p = 10$, $\tau_c = 200$, $\sigma^2 = -96$ dBm, and the communication bandwidth is 20 MHz bandwidth. The hardware impairment factor ϵ is set to 0, 0.05, and 0.1 based on the typical values of UE hardware impairments in LTE [38].

4.1 Uplink channel estimation

Figure 2 depicts the normalized MSE (NMSE) $\text{tr}(\boldsymbol{C}_{lk})/\text{tr}(\boldsymbol{R}_{lk})$ of the channel estimates as a function of the effective SNR p_k/σ^2 for various hardware impairment factors ϵ. Increasing the hardware impairment factor ϵ leads to a rise in NMSE, indicating that using non-ideal UE hardware may reduce channel estimation accuracy. At low SNR, hardware impairments have a negligible effect on channel estimation. However, they have a significant impact at high SNR. Additionally, error floors exist for channel estimation in the presence of high SNR and pilot contamination, with the error floor being raised by the hardware impairment level. The NMSE approaches the error floor if an effective SNR exceeds 30 dB with pilot contamination or 40 dB without pilot contamination. This means that increasing the SNR further will not have much impact on the channel estimation. The channel estimation error floor vanishes when there

is no pilot contamination and the hardware impairment factor ϵ equals 0. It indicates that error-free channel estimation may be accomplished using ideal hardware when the SNR is sufficiently high. With high SNR and no pilot contamination, non-ideal UE hardware also causes error floors. This is because the orthogonality of the pilot sequences is corrupted by distortions caused by non-ideal UE hardware, resulting in interference from all UEs. It can be seen that the UE hardware impairments dramatically reduce the channel estimation quality of the CF mMIMO network, which is a factor that cannot be ignored in network analysis and design.

4.2 Uplink spectral efficiency analysis

Figure 3 compares the uplink average sum SE of the simulation results based on Theorem 2 and the analytical results of Corollary 2 under different ϵ and L. Note that the simulation results are obtained through Monte Carlo simulations with 200 random locations of the AP-UE and 1000 channel realizations. It is observed that for different values of ϵ and L, the "simulation results" and the "analytical results" are consistent, which verifies the correctness of our derivation. In addition, it can be seen that the uplink average sum SE increases with the number of APs. The reason is that more APs imply higher spatial degrees of freedom to resist interference and fading. Similarly, Monte Carlo simulations based on Theorem 2 are used to evaluate the performance of the centralized CF mMIMO network with non-ideal UE hardware.

Figure 4 demonstrates the cumulative distribution function (CDF) for the uplink SE of each UE under different hardware impairment factors with pilot contamination ($K = 40$, $\tau_p = 10$) when employing MR, RZF, and MMSE combining schemes in the CF mMIMO network. At the 90% likely SE points, the MMSE scheme provides the highest SE under the same hardware impairment factor ϵ. In contrast, the MR scheme yields the lowest SE, and the recommended RZF scheme performs close to the optimal MMSE receive combining. Since the MMSE combining scheme can suppress interference from other UEs, it provides the highest SE. However, it is impossible for all UEs to have good channel conditions simultaneously in practice, so ignoring interference signals of other UEs may lead to a decrease in SE. MR has the lowest SE when inter-user interference is present, as a high degree of favorable propagation between all UEs cannot be guaranteed. Therefore, the MR combining led to a more significant loss of SE when compared to RZF and MMSE combining schemes. Increasing the hardware impairment level ϵ has substantially enhanced the SE of RZF and MMSE combining schemes, while UEs with high SE under MR combining are significantly affected. We observe that RZF with perfect hardware provides higher SE than MMSE with non-ideal UE hardware, indicating that UE hardware impairments must be considered while designing networks.

Figure 5 is a bar diagram illustrating the average uplink sum SE with three combining schemes under pilot contamination ($K = 40$, $\tau_p = 10$). As anticipated, adopting the MMSE combining scheme with ideal hardware results in the highest SE. If RZF combining is employed instead, SE is reduced by 4.88% with ideal hardware, 3.90% with hardware impairment factor ϵ of 0.05, and 3.38% with hardware impairment factor ϵ of 0.1. RZF can provide nearly the same SE as the MME combining scheme, while MR performs poorly. It is observed that improving the hardware quality brings little gain to the sum SE of the MR combining scheme.

Figure 6 illustrates the uplink SE for each UE with hardware impairments adopting the MMSE combining scheme for the presence ($K = 40$, $\tau_p = 10$) and absence ($K = 40$, $\tau_p = 40$) of pilot contamination. At the 90% likely SE points, the SE without pilot contamination is higher than that with pilot contamination under ideal hardware. However, the opposite is true when there are hardware impairments. This shows that compared with hardware impairments, the pilot sequence length τ_p has become the main factor affecting SE. In the case of hardware impairment factors of 0.05 and 0.1, the SE of most UEs is higher when the pilot length is 10 than when there is no pilot contamination, that is, $\tau_p = 40$. Compared with the pilot length of 10, the SE loss caused by the pre-log factor $\frac{\tau_u}{\tau_c}$ when the pilot length is 40 is greater than the gain brought by improving the channel estimation quality.

Figure 7 is a bar graph depicting the average sum SE under the presence ($K = 40$, $\tau_p = 10$) or absence ($K = 40$, $\tau_p = 40$) of pilot contamination. The highest SEs are obtained under ideal hardware without pilot contamination. Compared with the ideal hardware of pilot contamination, the case without pilot contamination improves SE by 6.98%, mainly due to the increase in pilot sequence length, which makes channel estimation more accurate. However, the case without pilot contamination loses 5.59% and 9.87% of SE compared to the pilot contamination with hardware impairments at a hardware impairment level of

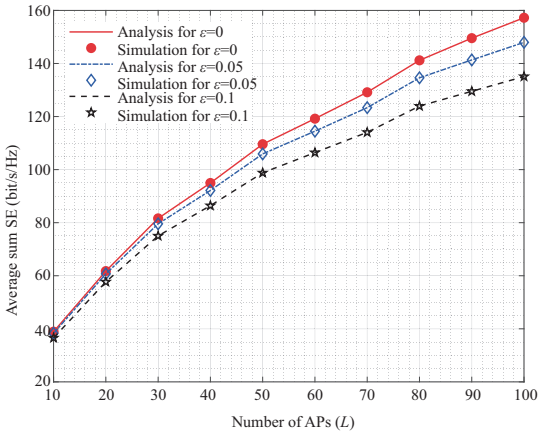

Figure 3 Average sum SE as a function of the number of APs L for different hardware impairment factors. We consider a CF mMIMO network with centralized operation and non-ideal UE hardware, where $K = 40$, $N = 4$, and $\tau_p = 10$.

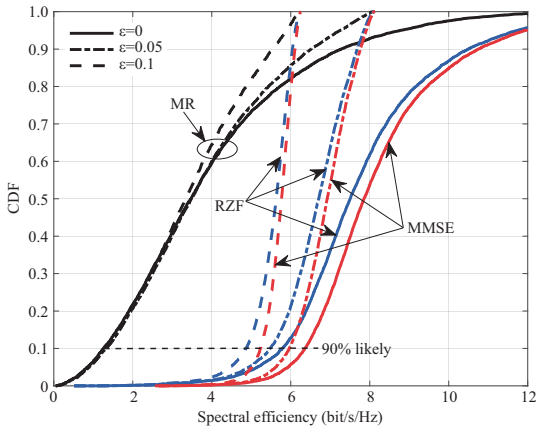

Figure 4 Uplink SE for each UE in a fully centralized processing CF mMIMO under different hardware impairment factors, using different combining schemes based on pilot contamination.

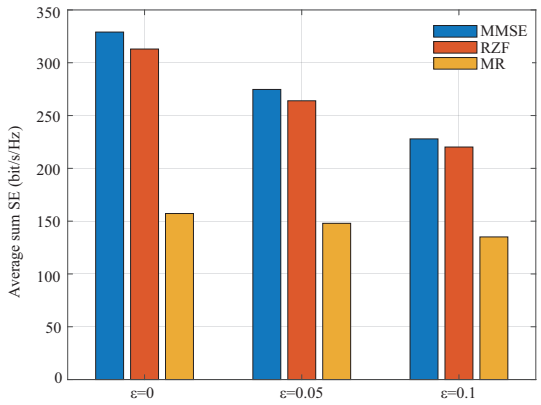

Figure 5 Average uplink sum SE of a fully centralized processing CF mMIMO network under different hardware impairment factors when utilizing three combining schemes based on pilot contamination.

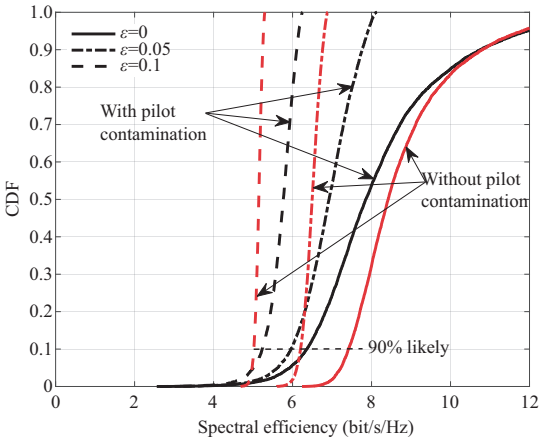

Figure 6 Uplink SE for each UE in a fully centralized processing CF mMIMO under different hardware impairment factors, using MMSE combining based on pilot contamination and no pilot contamination.

0.05 and 0.1, respectively. The main reason is that compared with the level of UE hardware impairments, the length of the pilot becomes the main factor affecting the SE. Therefore, how to design the length of the pilot in the CF mMIMO network with non-ideal UE hardware is very important.

Remark 1. The SINR can be improved by increasing the pilot length τ_p since it can enhance the accuracy of the channel estimate, and the pre-log factor $\frac{\tau_u}{\tau_c}$ decreases with τ_p. Therefore, it is crucial to determine the pilot length to maximize the SE. It is not straightforward to optimize the pilot sequence length given that lengthier pilots result in fewer data transmission samples. However, we expect to numerically optimize the pilot length τ_p to achieve the maximum SE.

4.3 Impact of the pilot length

Figure 8 demonstrates how the pilot length τ_p affects the average total SE under different hardware impairment factors. When K is kept fixed, a larger τ_p will lead to a reduction in pilot contamination and also a reduction in the pre-log factor $\frac{\tau_u}{\tau_c}$ in (14) due to the decrease in data samples available in each coherence block. For MMSE and RZF combining schemes, increasing the pilot sequence length can improve the average sum SE up to a certain point and then decay with τ_p. However, when τ_p grows, the total SE of the MR combining declines because the SE gain from the enhanced channel estimation quality is not more than the SE loss from decreasing the pre-log factor $\frac{\tau_u}{\tau_c}$. In the case of MMSE combining, the

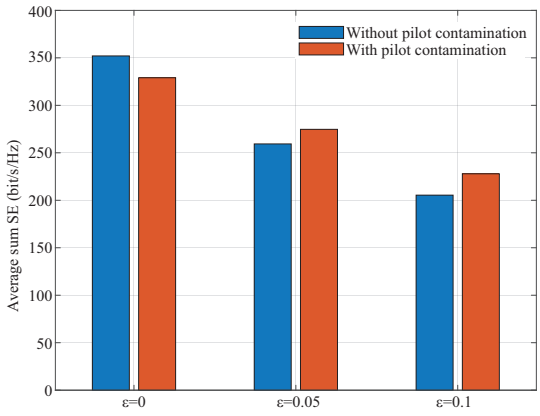

Figure 7 Average uplink sum SE for a fully centralized processing CF mMIMO under different hardware impairment factors when using MMSE combining based on the presence or absence of pilot contamination.

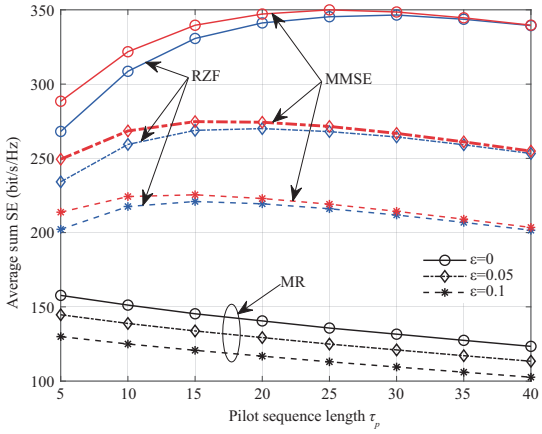

Figure 8 Average uplink sum SE for different combining schemes as a function of the pilot length τ_p, where the number of UEs is 40, and the pilot length gradually increases from 5 to 40.

average uplink sum SE gradually saturates as τ_p increases and τ_u samples set aside for data transmission on the uplink go down. For ideal hardware, the maximum value of the average sum SE is 349.97 bit/s/Hz when $\tau_p = 25$. When the pilot sequence length τ_p is 15, the maximum value of the average sum SE is 274.74 and 225.47 bit/s/Hz under hardware impairment levels of $\epsilon = 0.05$ and $\epsilon = 0.1$, respectively. Compared with the MMSE combining scheme, the recommended RZF combining has a modest sum SE loss. In the case of RZF combining, the pilot sequence length we should design for an ideal hardware network is 30, and the average sum SE is 346.50 bit/s/Hz. We designed optimal pilot sequence lengths of 20 and 15 under hardware impairment factors of $\epsilon = 0.05$ and $\epsilon = 0.1$, respectively. This corresponds to 270.04 and 220.94 bit/s/Hz for the maximum sum SE, respectively. Note that MR combining provides significantly lower SE than the other two combining schemes with interference suppression. However, the MR combining scheme has the lowest computational complexity and can give the SE in a closed form, which provides important insights for network analysis and design.

4.4 Uplink power control

Figure 9 exhibits the uplink SE per UE with hardware impairments using the max-min fairness and fractional power control schemes. At the 99% likely SE points, we observe that under the hardware impairment factor ϵ, the lower tails of the CDF curves for max-min fairness power control all begin with the most significant value compared to the fractional power control scheme. This is because max-min fairness optimizes the performance of the most unlucky UE at the expense of everyone else in the CF mMIMO network. When $v = -0.5$, our proposed fractional power control scheme with UE hardware impairments achieves almost the same SE for the most unfortunate UE without reducing the SE of other UEs in the entire network. Therefore, our proposed fractional power control technique with $v = -0.5$ under UE hardware impairments is a perfect choice in raising the SE of the most unlucky UE compared to the max-min fairness power control scheme.

Figure 10 is a bar graph of the average uplink sum SE in the centralized CF mMIMO with different hardware impairment factors under the max-min fairness and fractional power control schemes. As anticipated, the fractional power control scheme produced the highest SE, while the max-min fairness yielded the lowest average uplink sum SEs. The suggested power control scheme provides a 27.70% improvement in SE compared to the max-min fairness power control scheme for ideal hardware. The SE improved by 19.83% and 13.37% under hardware impairment factors of $\epsilon = 0.05$ and $\epsilon = 0.1$, respectively. Note that as the hardware impairment factor ϵ increases, the rise in SE decreases, indicating that hardware impairments become the main factor affecting SE compared to the performance gain boosted by power control.

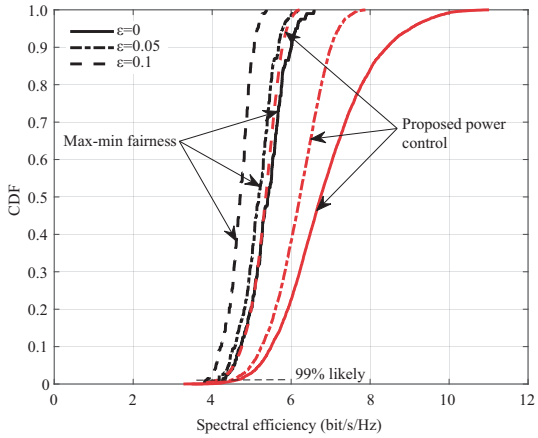

Figure 9 Uplink SE for each UE in a fully centralized processing CF mMIMO under different hardware impairment factors with the max-min fairness and fractional power control schemes.

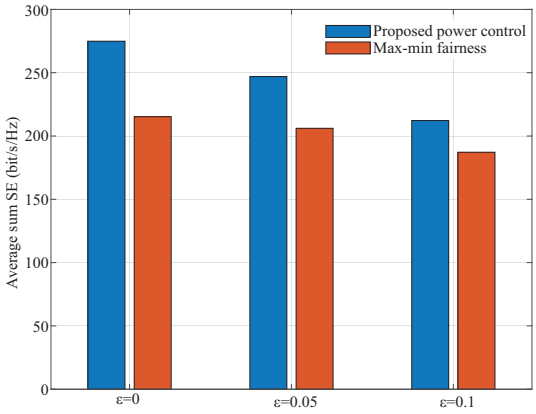

Figure 10 Average uplink sum SE in a fully centralized processing CF mMIMO under different hardware impairment factors with the max-min fairness and fractional power control schemes.

5 Conclusion and discussion

This paper has concentrated on the effects of non-ideal UE hardware on the performance of the CF mMIMO network with centralized operation. First, a well-established generic non-ideal UE hardware model is used to derive the MMSE channel estimator. It is shown that a non-zero estimate error floor is produced by pilot contamination and non-ideal UE hardware even though the effective SNR approaches infinity. The optimum combining scheme leading to the maximum instantaneous SINR is provided based on the lower bound on the ergodic uplink capacity. The MR and RZF combining schemes were provided regarding the computational complexity of the MMSE scheme, and the numerical results demonstrate that the RZF combining only loses the sum SE from 3.38% to 4.88% compared with the MMSE combining scheme, depending on the hardware impairment factor ϵ. Compared to the MMSE and RZF combining schemes, the MR scheme leads to a significant SE loss. Based on the uplink capacity lower bound derived using the bounding technique, a robust closed-form uplink SE expression can be obtained, which provides essential insights into the achievable uplink performance under UE hardware impairments, which can guide network design. The impact of pilot sequence length on average sum SE is investigated for different hardware impairment factors ϵ and three combining schemes. Compared to max-min SE fairness, our proposed fractional power control strategy with UE hardware impairments when $v = -0.5$ achieves almost the same SE for the unlucky UE without reducing the entire network SE for other UEs.

Acknowledgements This work was supported by National Natural Science Foundation of China (Grant No. 62020106001) and 111 Project (Grant No. 111-2-14).

References

1 Li N, Fan P Z. Impact of UE hardware impairments on uplink spectral efficiency of cell-free massive MIMO network. In: Proceedings of the IEEE Wireless Communications and Networking Conference (WCNC), 2023. 1–6
2 Marzetta T L. Noncooperative cellular wireless with unlimited numbers of base station antennas. IEEE Trans Wireless Commun, 2010, 9: 3590–3600
3 Larsson E G, Edfors O, Tufvesson F, et al. Massive MIMO for next generation wireless systems. IEEE Commun Mag, 2014, 52: 186–195
4 Andrews J G, Buzzi S, Choi W, et al. What will 5G be? IEEE J Sel Areas Commun, 2014, 32: 1065–1082
5 Parkvall S, Dahlman E, Furuskar A, et al. NR: the new 5G radio access technology. IEEE Comm Stand Mag, 2017, 1: 24–30
6 Bjornson E, Larsson E G, Debbah M. Massive MIMO for maximal spectral efficiency: how many users and pilots should be allocated? IEEE Trans Wireless Commun, 2016, 15: 1293–1308
7 Bjornson E, Hoydis J, Sanguinetti L. Massive MIMO has unlimited capacity. IEEE Trans Wireless Commun, 2018, 17: 574–590
8 Cai D H, Fan P Z, Zou Q Y, et al. Active device detection and performance analysis of massive non-orthogonal transmissions in cellular Internet of Things. Sci China Inf Sci, 2022, 65: 182301
9 Cheng G F, Chen H, Fan P Z, et al. A layered grouping random access scheme based on dynamic preamble selection for massive machine type communications. Sci China Inf Sci, 2022, 65: 179302
10 Ammar H A, Adve R, Shahbazpanahi S, et al. User-centric cell-free massive MIMO networks: a survey of opportunities, challenges and solutions. IEEE Commun Surv Tut, 2022, 24: 611–652
11 Elhoushy S, Ibrahim M, Hamouda W. Cell-free massive MIMO: a survey. IEEE Commun Surv Tut, 2022, 24: 492–523
12 Wang D M, You X H, Huang Y M, et al. Full-spectrum cell-free RAN for 6G systems: system design and experimental results. Sci China Inf Sci, 2023, 66: 130305

13 Bjornson E, Sanguinetti L. Making cell-free massive MIMO competitive with MMSE processing and centralized implementation. IEEE Trans Wireless Commun, 2020, 19: 77–90
14 Bjornson E, Sanguinetti L, Hoydis J. Hardware distortion correlation has negligible impact on UL massive MIMO spectral efficiency. IEEE Trans Commun, 2019, 67: 1085–1098
15 Bjornson E, Sanguinetti L, Kountouris M. Deploying dense networks for maximal energy efficiency: small cells meet massive MIMO. IEEE J Sel Areas Commun, 2016, 34: 832–847
16 Bjornson E, Hoydis J, Kountouris M, et al. Massive MIMO systems with non-ideal hardware: energy efficiency, estimation, and capacity limits. IEEE Trans Inform Theor, 2014, 60: 7112–7139
17 Zheng J K, Zhang J Y, Zhang L M, et al. Efficient receiver design for uplink cell-free massive MIMO with hardware impairments. IEEE Trans Veh Technol, 2020, 69: 4537–4541
18 Liu P, Luo K, Chen D, et al. Spectral efficiency analysis of cell-free massive MIMO systems with zero-forcing detector. IEEE Trans Wireless Commun, 2020, 19: 795–807
19 Rezaei F, Tellambura C, Tadaion A A, et al. Rate analysis of cell-free massive MIMO-NOMA with three linear precoders. IEEE Trans Commun, 2020, 68: 3480–3494
20 Nguyen H V, Nguyen V D, Dobre O A, et al. On the spectral and energy efficiencies of full-duplex cell-free massive MIMO. IEEE J Sel Areas Commun, 2020, 38: 1698–1718
21 Masoumi H, Emadi M J. Performance analysis of cell-free massive MIMO system with limited fronthaul capacity and hardware impairments. IEEE Trans Wireless Commun, 2020, 19: 1038–1053
22 Elhoushy S, Hamouda W. Performance of distributed massive MIMO and small-cell systems under hardware and channel impairments. IEEE Trans Veh Technol, 2020, 69: 8627–8642
23 Zhang Y, Zhang Q, Hu H, et al. Cell-free massive MIMO systems with non-ideal hardware: phase drifts and distortion noise. IEEE Trans Veh Technol, 2021, 70: 11604–11618
24 Zhang X Y, Guo D X, An K, et al. Secure communications over cell-free massive MIMO networks with hardware impairments. IEEE Syst J, 2020, 14: 1909–1920
25 Zhang X Y, Liang T, An K, et al. Secure transmission in cell-free massive MIMO with RF impairments and low-resolution ADCs/DACs. IEEE Trans Veh Technol, 2021, 70: 8937–8949
26 Papazafeiropoulos A, Bjornson E, Kourtessis P, et al. Scalable cell-free massive MIMO systems: impact of hardware impairments. IEEE Trans Veh Technol, 2021, 70: 9701–9715
27 Zhang Y, Zhou M, Cheng Y L, et al. RF impairments and low-resolution ADCs for nonideal uplink cell-free massive MIMO systems. IEEE Syst J, 2021, 15: 2519–2530
28 Hu X L, Zhong C J, Chen X M, et al. Cell-free massive MIMO systems with low resolution ADCs. IEEE Trans Commun, 2019, 67: 6844–6857
29 Björnson E, Hoydis J, Sanguinetti L. Massive MIMO networks: spectral, energy, and hardware efficiency. FNT Signal Process, 2017, 11: 154–655
30 Bjornson E, Sanguinetti L. Scalable cell-free massive MIMO systems. IEEE Trans Commun, 2020, 68: 4247–4261
31 Interdonato G, Björnson E, Ngo H Q, et al. Ubiquitous cell-free massive MIMO communications. J Wireless Com Netw, 2019, 2019(1): 197
32 Ngo H Q, Ashikhmin A, Yang H, et al. Cell-free massive MIMO versus small cells. IEEE Trans Wireless Commun, 2017, 16: 1834–1850
33 Nayebi E, Ashikhmin A, Marzetta T L, et al. Precoding and power optimization in cell-free massive MIMO systems. IEEE Trans Wireless Commun, 2017, 16: 4445–4459
34 Bashar M, Cumanan K, Burr A G, et al. On the uplink max-min SINR of cell-free massive MIMO systems. IEEE Trans Wireless Commun, 2019, 18: 2021–2036
35 Bashar M, Cumanan K, Burr A G, et al. Max-min rate of cell-free massive MIMO uplink with optimal uniform quantization. IEEE Trans Commun, 2019, 67: 6796–6815
36 Interdonato G, Karlsson M, Bjornson E, et al. Local partial zero-forcing precoding for cell-free massive MIMO. IEEE Trans Wireless Commun, 2020, 19: 4758–4774
37 Nikbakht R, Mosayebi R, Lozano A. Uplink fractional power control and downlink power allocation for cell-free networks. IEEE Wireless Commun Lett, 2020, 9: 774–777
38 Toskala A, Holma H. LTE for UMTS: Evolution to LTE-Advanced. 2nd ed. Hoboken: Wiley, 2011
39 Demir Ö T, Björnson E, Sanguinetti L. Foundations of user-centric cell-free massive MIMO. FNT Signal Process, 2021, 14: 162–472
40 Chen S, Zhang J, Bjornson E, et al. Structured massive access for scalable cell-free massive MIMO systems. IEEE J Sel Areas Commun, 2021, 39: 1086–1100
41 3GPP. Further advancements for E-UTRA physical layer aspects (Release 9). 3GPP TS 36.814, 2017

Appendix A Proof of Lemma 1

The pilot signal $\boldsymbol{y}_{lk}^p$ that has been received and processed is used to estimate $\boldsymbol{h}_{lk}$, so (5) can be rewritten as

$$\boldsymbol{y}_{lk}^p = \underbrace{\sqrt{p_k\left(1-\epsilon^2\right)}\tau_p\boldsymbol{h}_{lk}}_{\text{Desired pilot}} + \underbrace{\boldsymbol{N}_l^p\boldsymbol{\phi}_k^*}_{\text{Noise}} + \underbrace{\sum_{i=1}^{K}\boldsymbol{h}_{li}\boldsymbol{e}_i^{\mathrm{T}}\boldsymbol{\phi}_k^*}_{\text{Transmitter distortion}} + \underbrace{\sum_{i\in\mathcal{P}_k\setminus\{k\}}\sqrt{p_i\left(1-\epsilon^2\right)}\tau_p\boldsymbol{h}_{li}}_{\text{Interfering pilots}}. \tag{A1}$$

We get $q=\sqrt{p_k\left(1-\varepsilon^2\right)}\tau_p$ and $\boldsymbol{x}\sim\mathcal{N}_{\mathbb{C}}\left(0,\boldsymbol{R}_{lk}\right)$ after matching $\boldsymbol{y}=\boldsymbol{y}_{lk}^p$ to the structure in [29, Cor B.18], where the interference term is

$$\boldsymbol{n} = \sum_{i\in\mathcal{P}_k\setminus\{k\}}\sqrt{p_i\left(1-\epsilon^2\right)}\tau_p\boldsymbol{h}_{li} + \sum_{i=1}^{K}\boldsymbol{h}_{li}\boldsymbol{e}_i^{\mathrm{T}}\boldsymbol{\phi}_k^* + \boldsymbol{N}_l^p\boldsymbol{\phi}_k^*. \tag{A2}$$

By calculation, the interference vector $\boldsymbol{n}$ has zero mean, and the variance is

$$\boldsymbol{S} = \sum_{i\in\mathcal{P}_k\setminus\{k\}} p_i(1-\epsilon^2)\tau_p^2\boldsymbol{R}_{li} + \sum_{i=1}^{K}\epsilon^2 p_i\tau_p\boldsymbol{R}_{li} + \tau_p\sigma^2\boldsymbol{I}_N. \tag{A3}$$

The MMSE channel estimation $\hat{\boldsymbol{h}}_{lk}$ in (6) and the estimation error correlation matrix $\boldsymbol{C}_{lk}$ in (8) can be calculated directly with the help of [29, Cor B.18]. Note that the MMSE estimate $\hat{\boldsymbol{h}}_{lk}$ can minimize the MSE $\mathrm{tr}\left(\boldsymbol{C}_{lk}\right)$. The correlation matrix of $\boldsymbol{y}_{lk}^{p}$ is $\mathbb{E}\{\boldsymbol{y}_{lk}^{p}\left(\boldsymbol{y}_{lk}^{p}\right)^{\mathrm{H}}\}=\tau_{p}\boldsymbol{\Psi}_{lk}$. By directly calculating $\mathbb{E}\{\hat{\boldsymbol{h}}_{lk}\hat{\boldsymbol{h}}_{lk}^{\mathrm{H}}\}$, we can obtain the distribution of $\hat{\boldsymbol{h}}_{lk}$ as $\hat{\boldsymbol{h}}_{lk}\sim\mathcal{N}_{\mathbb{C}}\left(\boldsymbol{0},\boldsymbol{R}_{lk}-\boldsymbol{C}_{lk}\right)$. Since the MMSE estimator is used, $\hat{\boldsymbol{h}}_{lk}$ and $\tilde{\boldsymbol{h}}_{lk}$ are independent.

Appendix B Proof of Theorem 1

According to the notation defined in [29, Cor. 1.3], the input signal is $\sqrt{1-\epsilon^{2}}s_{k}$, and the channel response is $\boldsymbol{v}_{k}^{\mathrm{H}}\hat{\boldsymbol{h}}_{k}$ in (13), where the interference term is

$$i=\boldsymbol{v}_{k}^{\mathrm{H}}\tilde{\boldsymbol{h}}_{k}\sqrt{1-\epsilon^{2}}s_{k}+\sum_{i=1,i\neq k}^{K}\boldsymbol{v}_{k}^{\mathrm{H}}\boldsymbol{h}_{i}\sqrt{1-\epsilon^{2}}s_{i}+\sum_{i=1}^{K}\boldsymbol{v}_{k}^{\mathrm{H}}\boldsymbol{h}_{i}e_{i}+\boldsymbol{v}_{k}^{\mathrm{H}}\boldsymbol{n}. \tag{B1}$$

Note that the noise term is 0, The mean of the interfering signal i is 0, and the variance is

$$p_{i}=\mathbb{E}\{|i|^{2}\}=\boldsymbol{v}_{k}^{\mathrm{H}}\left(\sum_{i=1}^{K}p_{i}\left(\hat{\boldsymbol{h}}_{i}\hat{\boldsymbol{h}}_{i}^{\mathrm{H}}+\boldsymbol{C}_{i}\right)+\boldsymbol{Z}_{k}\right)\boldsymbol{v}_{k}, \tag{B2}$$

where

$$\boldsymbol{Z}_{k}=p_{k}\left(\epsilon^{2}-1\right)\hat{\boldsymbol{h}}_{k}\hat{\boldsymbol{h}}_{k}^{\mathrm{H}}+\sigma^{2}\boldsymbol{I}_{LN}. \tag{B3}$$

Note that p_i is equal to the denominator in (15). We take advantage of the fact that each zero-mean signal s_i is independent and the signal and channel are also independent, and the interference term is uncorrelated with the input signal because

$$\mathbb{E}\{s_{k}*i\}=\sqrt{1-\varepsilon^{2}}\mathbb{E}\{\boldsymbol{v}_{k}^{\mathrm{H}}\tilde{\boldsymbol{h}}_{k}\}\mathbb{E}\{|s_{k}|^{2}\}=0, \tag{B4}$$

where the second equation takes advantage of the fact that the estimation error $\tilde{\boldsymbol{h}}_{k}$ is uncorrelated with the channel estimate, and the signal s_k is independent of all terms in (B1) except the first one. Therefore, the achievable SE of UE k can be obtained in (14) by applying [29, Cor. 1.3]. Note that the pre-log factor τ_u/τ_c represents the proportion of channel usage allotted for uplink data transmission, which leads to SE in (14) being expressed in bit/s/Hz.

Appendix C Proof of Corollary 1

The SINR_k shown in (15) may also be represented as

$$\mathsf{SINR}_{k}=\frac{\left|\boldsymbol{v}_{k}^{\mathrm{H}}\boldsymbol{a}_{k}\right|^{2}}{\boldsymbol{v}_{k}^{\mathrm{H}}\boldsymbol{B}_{k}\boldsymbol{v}_{k}}, \tag{C1}$$

for a fixed vector $a_{k}=\sqrt{p_{k}\left(1-\epsilon^{2}\right)}\hat{\boldsymbol{h}}_{k}$ and a fixed matrix

$$\boldsymbol{B}_{k}=\sum_{i=1}^{K}p_{i}\left(\hat{\boldsymbol{h}}_{i}\hat{\boldsymbol{h}}_{i}^{\mathrm{H}}+\boldsymbol{C}_{i}\right)+\boldsymbol{Z}_{k}. \tag{C2}$$

Solved by writing (C1) in the generalized Rayleigh quotient [29, Lemma B.10], the maximum SINR becomes $\boldsymbol{a}_{k}^{\mathrm{H}}\boldsymbol{B}_{k}^{-1}\boldsymbol{a}_{k}$, which is calculated as given in (15). The lemma also offers $\boldsymbol{v}_{k}=\boldsymbol{B}_{k}^{-1}\boldsymbol{a}_{k}$ as a combining vector that achieves this maximum. Recall that

$$\boldsymbol{B}_{k}^{-1}\boldsymbol{a}_{k}=\left(1+\boldsymbol{a}_{k}^{\mathrm{H}}\boldsymbol{B}_{k}^{-1}\boldsymbol{a}_{k}\right)\left(\boldsymbol{B}_{k}+\boldsymbol{a}_{k}\boldsymbol{a}_{k}^{\mathrm{H}}\right)^{-1}\boldsymbol{a}_{k}, \tag{C3}$$

where $\left(1+\boldsymbol{a}_{k}^{\mathrm{H}}\boldsymbol{B}_{k}^{-1}\boldsymbol{a}_{k}\right)$ and $\sqrt{p_{k}\left(1-\epsilon^{2}\right)}$ are scalars. Since scaling $\boldsymbol{v}_k$ by any non-zero scalar does not change the value of SINR in (15), Eq. (17) is also the optimum combining scheme.

Appendix D Proof of Theorem 2

The CPU treats $\mathbb{E}\{\boldsymbol{v}_{k}^{\mathrm{H}}\boldsymbol{h}_{k}\}$ as a true deterministic channel because it has no knowledge of the channel estimates in (20). Hence the input signal is $\sqrt{1-\epsilon^{2}}s_{k}$, the channel response is $\mathbb{E}\{\boldsymbol{v}_{k}^{\mathrm{H}}\boldsymbol{h}_{k}\}$, and the interference term is

$$v=\sqrt{1-\epsilon^{2}}\sum_{i=1}^{K}\boldsymbol{v}_{k}^{\mathrm{H}}\boldsymbol{h}_{i}s_{i}-\sqrt{1-\epsilon^{2}}\mathbb{E}\{\boldsymbol{v}_{k}^{\mathrm{H}}\boldsymbol{h}_{k}\}s_{k}+\boldsymbol{v}_{k}^{\mathrm{H}}\boldsymbol{n}+\sum_{i=1}^{K}\boldsymbol{v}_{k}^{\mathrm{H}}\boldsymbol{h}_{i}e_{i}. \tag{D1}$$

Since the mean of the interference signal v is 0 and independent of the input signal, its variance is

$$p_{v}=\mathbb{E}\{|v|^{2}\}=\sum_{i=1}^{K}p_{i}\mathbb{E}\left\{\left|\boldsymbol{v}_{k}^{\mathrm{H}}\boldsymbol{h}_{i}\right|^{2}\right\}-\boldsymbol{D}_{k}+\sigma^{2}\mathbb{E}\{\|\boldsymbol{v}_{k}\|^{2}\}, \tag{D2}$$

where

$$\boldsymbol{D}_{k}=p_{k}\left(1-\epsilon^{2}\right)\left|\mathbb{E}\left\{\boldsymbol{v}_{k}^{\mathrm{H}}\boldsymbol{h}_{k}\right\}\right|^{2}. \tag{D3}$$

We take advantage of the fact that each zero-mean signal s_i is independent, and the signal and channel are also independent. The uplink lower bound capacity can be calculated directly and obtained in (21) with the help of [29, Cor B.18].

Appendix E Proof of Corollary 2

We use the properties of the MMSE estimator to directly compute the three expectations that appear in (22). First the expectation in the numerator term is computed as

$$\mathbb{E}\{\boldsymbol{v}_k^{\mathrm{H}}\boldsymbol{h}_k\} = \mathbb{E}\{\hat{\boldsymbol{h}}_k^{\mathrm{H}}\boldsymbol{h}_k\} = \mathbb{E}\{\hat{\boldsymbol{h}}_k^{\mathrm{H}}\hat{\boldsymbol{h}}_k\} = \mathrm{tr}(\mathbb{E}\{\hat{\boldsymbol{h}}_k\hat{\boldsymbol{h}}_k^{\mathrm{H}}\}) = p_k\left(1-\epsilon^2\right)\tau_p\sum_{l=1}^{L}\mathrm{tr}(\boldsymbol{R}_{lk}\boldsymbol{\Psi}_{lk}^{-1}\boldsymbol{R}_{lk}). \tag{E1}$$

Since $\mathbb{E}\{\|\boldsymbol{v}_k\|^2\} = \mathrm{tr}(\mathbb{E}\{\hat{\boldsymbol{h}}_k\hat{\boldsymbol{h}}_k^{\mathrm{H}}\})$, the expectation in (25) is also calculated as

$$\mathbb{E}\{\|\boldsymbol{v}_k\|^2\} = p_k\left(1-\epsilon^2\right)\tau_p\sum_{l=1}^{L}\mathrm{tr}(\boldsymbol{R}_{lk}\boldsymbol{\Psi}_{lk}^{-1}\boldsymbol{R}_{lk}). \tag{E2}$$

According to whether or not $i \in \mathcal{P}_k$, the interference term in (26) is calculated in two parts. In the case of $i \notin \mathcal{P}_k$, we can obtain

$$\mathbb{E}\{\left|\boldsymbol{v}_k^{\mathrm{H}}\boldsymbol{h}_i\right|^2\} = \mathbb{E}\{\hat{\boldsymbol{h}}_k^{\mathrm{H}}\boldsymbol{h}_i\boldsymbol{h}_i^{\mathrm{H}}\hat{\boldsymbol{h}}_k\} = \mathrm{tr}\left(\mathbb{E}\{\boldsymbol{h}_i\boldsymbol{h}_i^{\mathrm{H}}\}\mathbb{E}\{\hat{\boldsymbol{h}}_k\hat{\boldsymbol{h}}_k^{\mathrm{H}}\}\right) = p_k\left(1-\epsilon^2\right)\tau_p\sum_{l=1}^{L}\mathrm{tr}\left(\boldsymbol{R}_{li}\boldsymbol{R}_{lk}\boldsymbol{\Psi}_{lk}^{-1}\boldsymbol{R}_{lk}\right). \tag{E3}$$

In the case of $i \in \mathcal{P}_k$, we can obtain

$$\mathbb{E}\{\left|\boldsymbol{v}_k^{\mathrm{H}}\boldsymbol{h}_i\right|^2\} = \mathbb{E}\left\{\hat{\boldsymbol{h}}_k^{\mathrm{H}}(\hat{\boldsymbol{h}}_i+\tilde{\boldsymbol{h}}_i)(\hat{\boldsymbol{h}}_i+\tilde{\boldsymbol{h}}_i)^{\mathrm{H}}\hat{\boldsymbol{h}}_k\right\} = \mathbb{E}\{\hat{\boldsymbol{h}}_k^{\mathrm{H}}\hat{\boldsymbol{h}}_i\hat{\boldsymbol{h}}_i^{\mathrm{H}}\hat{\boldsymbol{h}}_k\} + \mathbb{E}\{\hat{\boldsymbol{h}}_k^{\mathrm{H}}\tilde{\boldsymbol{h}}_i\tilde{\boldsymbol{h}}_i^{\mathrm{H}}\hat{\boldsymbol{h}}_k\}. \tag{E4}$$

Note that $\hat{\boldsymbol{h}}_k = \sqrt{p_k\left(1-\epsilon^2\right)}\boldsymbol{R}_k\boldsymbol{\Psi}_k^{-1}\boldsymbol{y}_k^p$ and $\hat{\boldsymbol{h}}_i = \sqrt{p_i\left(1-\epsilon^2\right)}\boldsymbol{R}_i\boldsymbol{\Psi}_k^{-1}\boldsymbol{y}_k^p$, where the processed received pilot signals are collected in $\boldsymbol{y}_k^p = [(\boldsymbol{y}_{1k}^p)^{\mathrm{T}},\ldots,(\boldsymbol{y}_{Lk}^p)^{\mathrm{T}}]^{\mathrm{T}}$ and distributed as $\boldsymbol{y}_k^p \sim \mathcal{N}_{\mathbb{C}}\left(0,\tau_p\boldsymbol{\Psi}_k\right)$. Consequently, the first term of (E4) is calculated as

$$\mathbb{E}\{\hat{\boldsymbol{h}}_k^{\mathrm{H}}\hat{\boldsymbol{h}}_i\hat{\boldsymbol{h}}_i^{\mathrm{H}}\hat{\boldsymbol{h}}_k\} = p_kp_i\left(1-\epsilon^2\right)^2\tau_p^2\left|\mathrm{tr}\left(\boldsymbol{R}_i\boldsymbol{\Psi}_k^{-1}\boldsymbol{R}_k\right)\right|^2 + p_k\left(1-\epsilon^2\right)\tau_p\mathrm{tr}\left(\left(\boldsymbol{R}_i-\boldsymbol{C}_i\right)\boldsymbol{R}_k\boldsymbol{\Psi}_k^{-1}\boldsymbol{R}_k\right). \tag{E5}$$

We now calculate the second term in (E4)

$$\mathbb{E}\{\hat{\boldsymbol{h}}_k^{\mathrm{H}}\tilde{\boldsymbol{h}}_i\tilde{\boldsymbol{h}}_i^{\mathrm{H}}\hat{\boldsymbol{h}}_k\} = \mathrm{tr}\left(\mathbb{E}\left\{\tilde{\boldsymbol{h}}_i\tilde{\boldsymbol{h}}_i^{\mathrm{H}}\right\}\mathbb{E}\left\{\hat{\boldsymbol{h}}_k\hat{\boldsymbol{h}}_k^{\mathrm{H}}\right\}\right) = p_k\left(1-\epsilon^2\right)\tau_p\mathrm{tr}\left(\boldsymbol{C}_i\boldsymbol{R}_k\boldsymbol{\Psi}_k^{-1}\boldsymbol{R}_k\right). \tag{E6}$$

By substituting (E5) and (E6) into (E4), we finally obtain

$$\begin{aligned}\mathbb{E}\left\{\left|\boldsymbol{v}_k^{\mathrm{H}}\boldsymbol{h}_i\right|^2\right\} &= p_kp_i\left(1-\epsilon^2\right)^2\tau_p^2\left|\mathrm{tr}\left(\boldsymbol{R}_i\boldsymbol{\Psi}_k^{-1}\boldsymbol{R}_k\right)\right|^2 + p_k\left(1-\epsilon^2\right)\tau_p\mathrm{tr}\left(\boldsymbol{R}_i\boldsymbol{R}_k\boldsymbol{\Psi}_k^{-1}\boldsymbol{R}_k\right)\\ &= p_kp_i\left(1-\epsilon^2\right)^2\tau_p^2\left|\sum_{l=1}^{L}\mathrm{tr}\left(\boldsymbol{R}_{li}\boldsymbol{\Psi}_{lk}^{-1}\boldsymbol{R}_{lk}\right)\right|^2 + p_k\left(1-\epsilon^2\right)\tau_p\sum_{l=1}^{L}\mathrm{tr}\left(\boldsymbol{R}_{li}\boldsymbol{R}_{lk}\boldsymbol{\Psi}_{lk}^{-1}\boldsymbol{R}_{lk}\right).\end{aligned} \tag{E7}$$

The $\underline{\mathsf{SINR}}_k$ expression in (27) can be obtained by substituting (24)–(26) into (22) and dividing both the numerator and denominator by $p_k(1-\epsilon^2)\tau_p d$.